Journal of Fluorescence
https://doi.org/10.1007/s10895-025-04543-0

RESEARCH

Comparative Evaluation of Benzimidazole-Based Schiff Bases as Fluorescent Probes for the Sensitive and Selective Detection of Cu^{2+} Ions in Water Samples

Zafer Ocak[1] · Abidin Gümrükçüoğlu[2] · Miraç Ocak[3] · Ümmühan Turgut Ocak[3]

Received: 7 July 2025 / Accepted: 12 August 2025

Abstract
A new spectrofluorimetric method has been developed for the selective detection of Cu^{2+} ions based on a benzimidazole-containing Schiff base ligand. In this study, three structurally related Schiff bases (L1, L2, and L3) were synthesized and comparatively investigated for their fluorescence response in the presence of various cations. Among them, only L3 bearing ortho-hydroxyl groups on the aromatic rings exhibited a notable fluorescence quenching effect upon interaction with Cu^{2+}, while L1 (para-hydroxyl substituted) and L2 (N, N-dimethylamino substituted) showed limited or no selectivity. The structure–function relationship revealed that the spatial orientation of donor groups plays a key role in metal coordination and signal transduction. The proposed method good sensitivity and selectivity toward Cu^{2+}, with a linear response in the concentration range of 0–32 µg/L and a low detection limit of 0.98 µg/L, enabling quantification at relatively low concentrations. Furthermore, the method was tested with tap water samples. This work offers a potentially useful approach for Cu^{2+} determination but also highlights the importance of ligand geometry in fluorescent probe design.

Keywords Cu^{2+} ion detection · Spectrofluorimetry · Benzimidazole · Schiff base ligand · Fluorescent sensor · Selectivity

Introduction

Benzimidazole and its derivatives have been widely studied in recent years owing to their diverse biological properties, distinct structural features, and potential applications in pharmaceutical development, materials science, and coordination chemistry [1, 2]. Featuring a fused benzene–imidazole ring system, benzimidazole presents a relatively rigid and planar framework with multiple coordination sites for hydrogen bonding, π–π stacking, and metal ion complexation, which makes it a useful structural motif in drug design and supramolecular chemistry [3, 4].

Cu^{2+} ions play essential roles in biological systems but can become toxic at elevated levels [5–9]. They function as catalytic cofactors in redox reactions and are involved in fundamental physiological processes such as iron metabolism and neurotransmitter synthesis. However, elevated concentrations of Cu^{2+} ions may contribute to oxidative stress, cellular damage, and have been associated with neurodegenerative disorders [10, 11]. Additionally, Cu^{2+} accumulation in the environment, often originating from industrial waste and agricultural activities, may pose risks to ecosystems and human health [12, 13]. Therefore, monitoring copper levels in clinical and environmental contexts is of significant concern [14, 15].

Among various analytical techniques employed, spectrofluorimetric methods are widely utilized due to favorable properties such as high sensitivity, relatively low detection limits, and operational simplicity [16, 17]. These methods have shown effectiveness particularly when based on fluorescence changes arising from the coordination of metal ions

✉ Zafer Ocak
zafcak@gmail.com

[1] Faculty of Education, Department of Mathematics and Science Education, Kafkas University, 36040 Kars, Türkiye

[2] Medicinal-Aromatic Plants Application and Reseach Center, Artvin Çoruh University, Artvin, Türkiye

[3] Faculty of Science, Department of Chemistry, Karadeniz Technical University, Trabzon 61080, Türkiye, Turkey

Published online: 04 September 2025

with organic ligands [18–21]. Schiff bases containing conjugated systems and heterocyclic units such as benzimidazole are commonly utilized as fluorescent probes, owing to their well-documented coordination ability and photophysical characteristics.

While various Schiff base systems, such as imidazole- and benzimidazole-based probes, have reported selective fluorescence responses to Cu^{2+}, this study focuses on a comparative structural screening of closely related derivatives. For instance, the Schiff base derived from 5,5′-methylene-bis-salicylaldehyde and amidol has been shown to exhibit fluorescence enhancement in the presence of Cu^{2+} with reported selectivity over other metal ions [22]. Similarly, a naphthalimide compound has demonstrated Cu^{2+} selectivity and relatively low detection limits in real samples [23].

Here, we systematically evaluated the spectrofluorimetric behavior of three benzimidazole-based Schiff base ligands (L1, L2, and L3) previously described in the literature [24, 25]. L1 is a bis(phenol)-substituted Schiff base with hydroxyl groups at para positions relative to the imine bonds. L2 contains two electron-donating N, N-dimethylamino groups within its aromatic framework. L3 features hydroxyl groups at ortho positions with respect to the imine linkages, which may allow intramolecular hydrogen bonding and result in a more preorganized geometry that could be favorable for metal ion coordination.

Although all three ligands share a common benzimidazole–Schiff base framework and potential chelation sites, only L3 showed notable and selective fluorescence response to Cu^{2+}. This suggests the significant influence of donor group positioning on metal–ligand interactions and suggests that ortho-hydroxyl substitution may be particularly effective for selective Cu^{2+} sensing. Our optimized spectrofluorimetric method based on L3 demonstrated good selectivity, low detection limits, and applicability in real sample matrices. These findings deepen our understanding of how subtle structural variations in benzimidazole-Schiff base ligands can impact selectivity and sensing performance.

Materials and Methods

Chemicals and Reagents

All chemicals used in this study were of analytical grade and utilized without further purification. Standard solutions of cations (1000 mg/L) were purchased from Merck. The organic reagents o-phenylenediamine, 2-hydroxybenzaldehyde, 4-hydroxybenzaldehyde, and 4-(dimethylamino) benzaldehyde were also obtained from Merck. Solvents such as ethanol, acetone, acetonitrile, N,N-dimethylformamide (DMF), dimethyl sulfoxide (DMSO), petroleum ether, benzene, and methanol were purchased from Sigma-Aldrich. Montmorillonite K10 clay was likewise obtained from Sigma-Aldrich. Deionized water used throughout the experiments was produced using a Merck Millipore Direct-Q 8 UV purification system.

Instrumentation

The synthesized ligands were characterized by melting point measurements, FT-IR spectroscopy (PerkinElmer spectrophotometer), and ^{1}H-NMR spectroscopy (Agilent 400/54 Annual Refill). Fluorescence spectra were recorded on a PTI QM-4-2006 spectrofluorometer using 1 cm quartz cuvettes. UV–vis absorption spectra were acquired using a Perkin Elmer Lambda 25 spectrophotometer. All spectroscopic measurements were conducted at room temperature (25 ± 1 °C).

Synthesis and Characterization of Ligands

o-Phenylenediamine was dissolved in ethanol and heated at 115 °C in a two-neck round-bottom flask equipped with a reflux condenser. Upon reaching reflux, the corresponding benzaldehyde derivative was added, and the reaction continued under reflux for 18 h. Progress was monitored by TLC (petroleum ether: ethanol: benzene, 1:1:1). After completion, the solvent was partially removed by rotary evaporation, and the mixture was refrigerated for 24 h. The resulting solid was filtered and dried under vacuum. The melting points, IR and ^{1}H NMR analyses confirmed the structures. Spectral and melting point data were consistent with literature values [24, 25].

- L1: Pale yellow solid. mp 229–231 °C. IR (KBr) cm^{-1}: 3248, 3050, 2923, 1593, 1440, 1241. 1 H-NMR, δ: 5.42 (2 H, CH_2, s), 6.67 (d, 2 H, Ar-H), 6.82 (d, 2 H, Ar-H), 6.91 (d, 2 H, Ar-H), 7.20 (m, 2 H, Ar-H), 7.53 (d, 2 H, Ar-H), 7.57 (d, 2 H, Ar-H), 9.57 (1 H, OH, s), 9.89 (1 H, OH, s).
- L2: Pale yellow solid. mp 235–238 °C. IR (KBr) cm^{-1}: 3030, 2851, 1607, 1438, 1199. 1 H-NMR, δ: 2.93–3.12 (s, 12 H, CH_3), 5.40 (2 H, CH_2 s), 6.65–7.80 (12 H, m, ArH).
- L3: Yellow solid. mp 209–212 °C. IR (KBr) cm^{-1}: 3318, 3057, 2920, 1590, 1452, 1237. 1 H-NMR, δ: 5.46 (2 H, CH_2, s), 6.5–8.1 (m, 12 H, Ar-H), 9.77 (1 H, OH, s), 11.2 (1 H, OH, s).

Preparation of Solutions

To determine the most suitable solvent for the ligands, water-miscible solvents including acetone, acetonitrile, ethanol,

methanol, tetrahydrofuran (THF), N,N-dimethylformamide (DMF), and dimethyl sulfoxide (DMSO) were evaluated. Among these, ethanol was identified as the optimal solvent for L1 and L3, while acetonitrile was selected for L2. For the metal ion solutions, DMSO was used with L1 due to solubility issues in aqueous media, whereas aqueous media were employed for L2 and L3, which exhibited sufficient water solubility. An ethanol–water (1:1, v/v) mixture was used as the most suitable solvent system for compound L3, which exhibited the best sensor properties for Cu^{2+} detection, providing both good solubility and strong fluorescence characteristics. Working solutions for the ligands were freshly prepared by diluting the stocks in relevant solvent. A series of solutions with concentrations ranging from 1×10^{-5} to 1×10^{-9} M were prepared to optimize the working ligand concentration. Optimal ligand concentrations were defined based on the maximum observed fluorescence intensity and determined to be 1.0×10^{-9} M, 2.0×10^{-8} M, and 2.5×10^{-8} M for L1, L2, and L3, respectively. In the titration experiments, metal ion and ligand solutions were mixed in a 1:1 volumetric ratio.

Fluorescence Measurements

Fluorescence measurements assessing the influence of various cations on the emission spectra of the ligands were conducted using metal ion concentrations at 100-fold excess relative to the ligand concentrations. This approach allowed for the identification of the metal ion causing significant changes in the ligand's fluorescence spectrum, thereby establishing selectivity.

Since only ligand L3 exhibited selective interaction with Cu^{2+} ions among the tested ligands, spectrofluorimetric titrations were performed using this compound. A series of solutions with ligand-to-metal (L/M) molar ratios ranging from 0 to 20 were prepared. After 5 min of equilibration fluorescence spectra were recorded upon excitation at 330 nm. For these experiments, a 2.5×10^{-8} M solution of L3 in ethanol and a 5.0×10^{-7} M aqueous solution of Cu^{2+} were used.

Cu^{2+} Determination Method

A modified standard addition method was used for the determination of Cu^{2+} in spiked tap water samples using compound L3 [26, 27]. For this purpose, 2 mL of an ethanolic solution of L3 (5×10^{-8} M) was added to each test tube. Subsequently, appropriate volumes of a Cu^{2+} standard solution was added to achieve a final Cu^{2+} concentration of 2 µg/L in each tube. Starting from the second tube, equal volumes of spiked tap water samples were added. From the third tube onwards, incremental volumes of the Cu^{2+} standard solution were further added. Finally, the volume in each tube was made up to 4 mL with ethanol. Fluorescence spectra were recorded upon excitation at 330 nm. The emission intensities at 449 nm were then plotted against the corresponding Cu^{2+} concentrations to construct a calibration curve. The Cu^{2+} concentration in the water sample was calculated according to Eq. 1.

Results and Discussion

Synthesis and Characterization of Ligands

The Schiff base ligands (L1, L2, and L3) were synthesized according to the common procedure [24, 25]. The structures of the prepared Schiff bases are given in Scheme 1.

o-phenylenediamine was used as the amine compound. As the aldehyde compound, 4-hydroxy benzaldehyde was used for L1, 4-(dimethylamino)benzaldehyde for L2, and 2-hydroxybenzaldehyde for L3. The reactions were carried out by boiling the *o*-phenylenediamine compound with the relevant aldehyde compound in ethanol for 18 h. The melting points, FTIR and 1 H NMR spectral data of the Schiff bases were found to be consistent with the literature [24, 25]. The characteristic imine (C = N) proton signal appeared in the range of 8.2–8.6 ppm in the ^{1}H NMR spectra. In the IR spectra, the C = N stretching vibration was observed near 1610–1625 cm^{-1}.

Scheme 1 Structures of benzimidazole-based Schiff bases, L1, L2, and L3

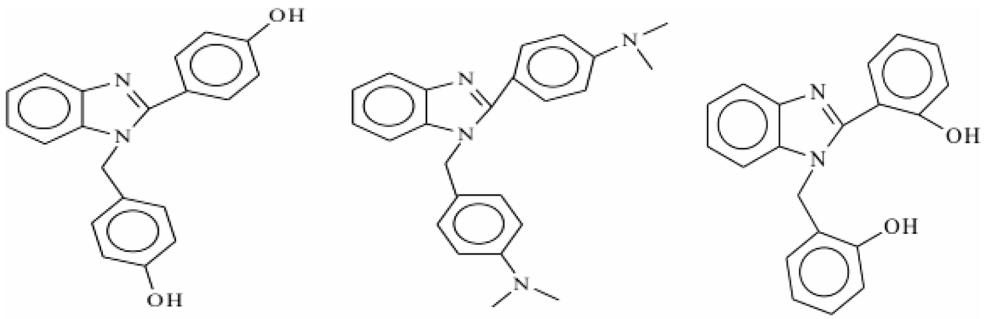

Fluorescence Behavior of Ligands in the Presence of Cations

The interaction of ligands with various cations was studied by monitoring the changes in their fluorescence spectrum. The cations studied included: Pd^{2+}, Fe^{3+}, Al^{3+}, Ni^{2+}, V^{5+}, Mn^{2+}, Mg^{2+}, Ca^{2+}, Bi^{3+}, Sc^{2+}, Cd^{2+}, Cr^{3+}, Be^{2+}, Cu^{2+}, Co^{2+}, Hg^{2+}, Ag^{+}, Sb^{3+}, As^{3+}, Sr^{2+}, Sn^{2+}, Ba^{2+}, Na^{+}, Li^{+}, Zn^{2+}, and K^{+}.

The fluorescence response of the Schiff base compound L1 in the presence of different cations was evaluated to investigate its potential as a fluorescent chemosensor. As shown in Figure S1a, L1 displayed a strong emission peak centered at approximately 350 nm. Upon addition of a wide range of cations (including Mg^{2+}, Ba^{2+}, Pb^{2+}, Pd^{2+}, Fe^{3+}, Sb^{3+}, Sn^{2+}, Na^{+}, Mn^{2+}, Zn^{2+}, Cd^{2+}, Co^{2+}, Ag^{+}, Hg^{2+}, Cu^{2+}, Al^{3+}, Yb^{3+}, Ca^{2+}, and others), the emission spectra of L1 remained largely unchanged in terms of both intensity and shape. As can be seen in Figure S1b, the fluorescence intensity of L1 at 350 nm was not markedly influenced by the presence of any of the tested cations. Although slight fluctuations in intensity were observed (e.g., mild quenching by Mn^{2+} and slight enhancement by V^{5+} or Li^{+}), these changes were relatively minor and not selective to any specific ion. This result suggests that L1 does not exhibit significant or selective interaction with these cations under the experimental conditions employed. The fluorescence stability of L1 in the presence of a variety of cations indicates its limited applicability for selective cation sensing. However, the negligible quenching across nearly all tested cations may suggest a potential advantage for L1 in applications where fluorescence stability in complex ionic environments is desirable.

The impact of various cations on the fluorescence characteristics of the Schiff base compound L2 was investigated to explore its potential use in cation sensing applications. As depicted in Figure S2a, L2 exhibits a strong emission maximum around 385 nm. Upon addition of different cations, including transition metals, alkali and alkaline earth metals, and post-transition metals, the fluorescence spectra of L2 generally maintained their shape, with some variations in intensity. The fluorescence intensity at 385 nm, summarized in the bar graph (Figure S2b), shows that certain cations caused moderate changes such as enhancement or quenching. Notably, Fe^{3+}, Pd^{2+}, and Bi^{3+} induced a measurable fluorescence enhancement compared to the free L2 ligand. In contrast, the presence of other cations resulted in a less pronounced enhancement of fluorescence intensity. These results suggest that L2 is less selective and less strongly responsive to individual cations. The moderate changes in fluorescence signal can be attributed to differing degrees of interaction between L2 and the added cations. The enhancement observed with Fe^{3+} and Pd^{2+} may be due to the formation of rigid complexes that reduce nonradiative decay pathways. Overall, while L2 shows some degree of responsiveness to specific cations, the fluorescence intensity changes are relatively modest and do not indicate a single highly selective target. Therefore, L2 may serve as a general probe for the presence of cations, but further structural tuning may be necessary to achieve high selectivity and sensitivity toward a particular analyte.

The influence of various cations on the fluorescence behavior of L3 was systematically investigated to assess its potential as a fluorescent sensor with selectivity toward Cu^{2+} ions. As shown in Fig. 1a, the free L3 displayed a strong fluorescence emission centered at 449 nm. Upon addition of different cations, the emission profiles were generally maintained with minimal changes in intensity except for Cu^{2+}. The presence of Cu^{2+} caused noticeable quenching of the fluorescence intensity of L3. This effect is clearly seen in both the emission spectra (Fig. 1a) and in the bar graph showing fluorescence intensity at 449 nm (Fig. 1b).

The quenching effect caused by Cu^{2+} is more pronounced than that of any other cation tested, indicating a notable degree of selectivity of L3 toward copper ions. This fluorescence quenching is likely attributed to the paramagnetic nature of Cu^{2+} (d^9 configuration), which may facilitate nonradiative deactivation pathways and thereby reduces the emission [28, 29]. The strong interaction between L3 and Cu^{2+} is proposed to result in the formation of a non-emissive or weakly emissive complex, disrupting the π–π^* transition responsible for fluorescence [30, 31]. These findings suggest that L3 exhibits a degree of selectivity and sensitivity toward Cu^{2+} ions in the presence of various competing cations, indicating its potential suitability for environmental or biological sensing applications related to copper detection.

Effect of Ligand Structure on Interaction with Cations

The fluorescence behavior of the three synthesized Schiff base compounds (L1, L2, and L3) was systematically compared to evaluate their selectivity toward various cations. The data presented in Figures S1–S2 and Fig. 1 show distinct differences in their fluorescence responses, which may be attributed to structural variations affecting their sensing capabilities.

L1 exhibited relatively high fluorescence intensity centered around 350 nm, and its emission profile remained largely unaffected in the presence of a wide range of cations. The minimal changes in fluorescence intensity at 350 nm (Figure S1b) indicate that L1 does not show significant selective interaction with any cations. This suggests a limited binding environment or poor chelation ability under the tested conditions [32]. Therefore, L1 may not be suitable for

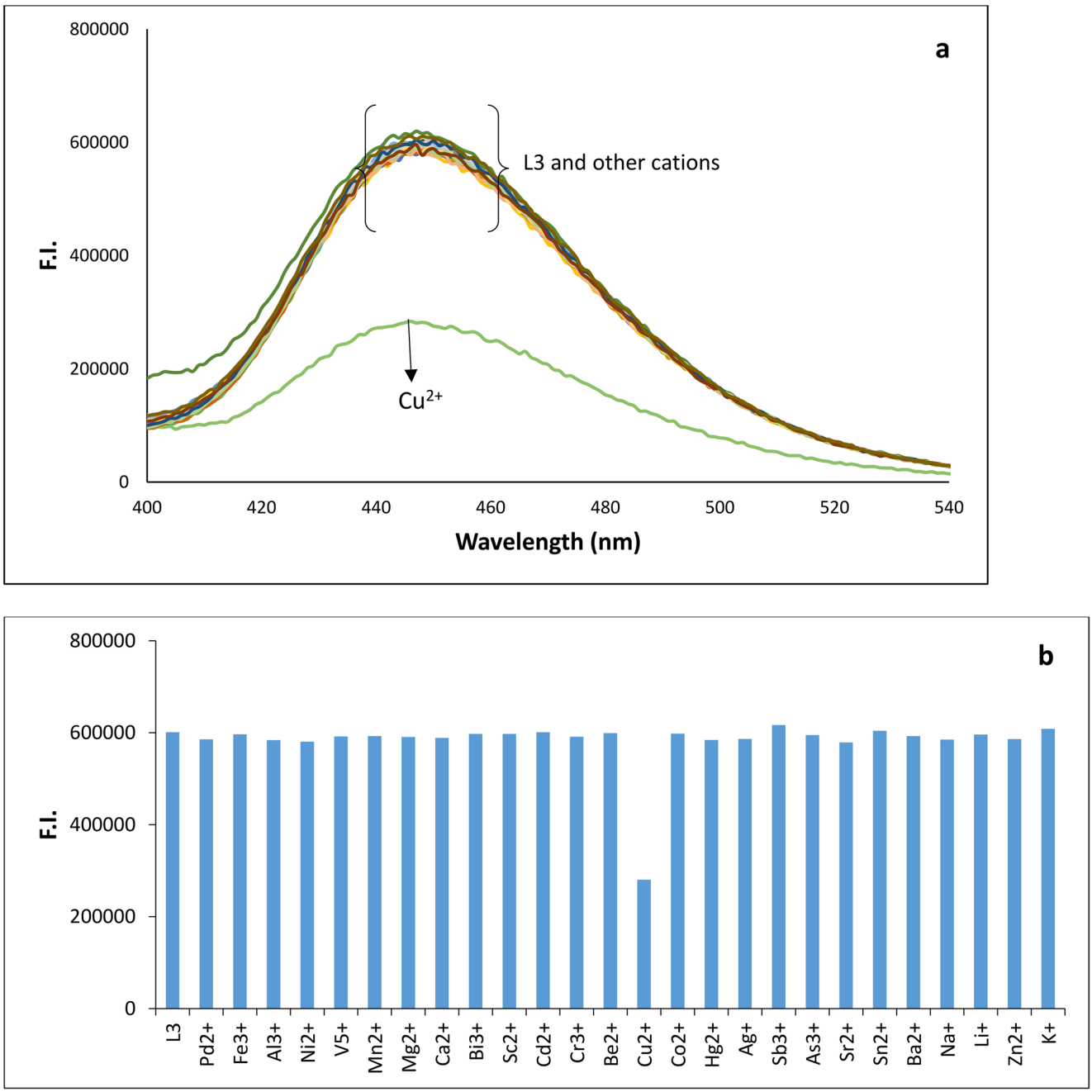

Fig. 1 Effect of cations on fluorescence spectra of L3 (**a**), change of fluorescence intensity with cations at 449 nm (**b**)

selective cation sensing but could serve as a comparatively stable fluorophore in multi-component systems.

In contrast, L2 displayed fluorescence emission around 385 nm and showed moderate changes in intensity with different cations (Figure S2b). While no single cation induced drastic fluorescence changes, Fe^{3+}, Bi^{3+}, and Pd^{2+} caused noticeable enhancement. These results suggest that L2 exhibits limited sensitivity to certain transition metal ions, potentially due to partial complex formation affecting the fluorophore's rigidity or electronic environment [33]. However, the lack of a distinct and selective response limits its use for targeted metal ion detection.

L3, on the other hand, showed a noticeable and relatively selective fluorescence quenching effect in the presence of Cu^{2+} ions (Fig. 1a and b). While other cations had minimal impact on the emission at 449 nm, Cu^{2+} caused a marked reduction in fluorescence intensity. This behavior is likely related to the structural features of L3, which contains a 2-hydroxybenzylidene moiety capable of forming a more stable chelate with Cu^{2+} through both the imine nitrogen and

the ortho-hydroxyl oxygen atom. The ortho-hydroxy substituent in L3 may facilitates the formation of a five-membered chelate ring with Cu^{2+}, enhancing the binding affinity and leading to an efficient quenching mechanism, possibly through photoinduced electron transfer (PET) or a ligand-to-metal charge transfer (LMCT) process [34]. In contrast, L1 and L2 lack such an optimal chelating arrangement; the para-hydroxy group in L1 and the electron-donating dimethylamino group in L2 do not appear to promote effective coordination with Cu^{2+} under the same conditions [35].

These results indicate the crucial influence of ligand geometry and donor atom positioning on metal ion recognition and photophysical behavior [36]. The selective and notable fluorescence quenching observed for L3 in the presence of Cu^{2+} suggests its potential utility as a sensitive and selective fluorescent sensor for Cu^{2+} ions in environmental or biological systems.

Proposed Method for Cu^{2+} Determination Using L3

After it was determined that Cu^{2+} causes a selective and measurable fluorescence quenching in L3, spectrofluorometric titration experiments were performed using this compound. Solutions with varying $[Cu^{2+}]/[L3]$ ratios were prepared, and their fluorescence spectra were recorded upon excitation at 330 nm. Figure 2 shows the results of the spectrofluorometric titration experiments.

As seen in Fig. 2a, the fluorescence intensity of L3 gradually decreases in a concentration-dependent manner upon addition of Cu^{2+} ions in the range of $[Cu^{2+}]/$

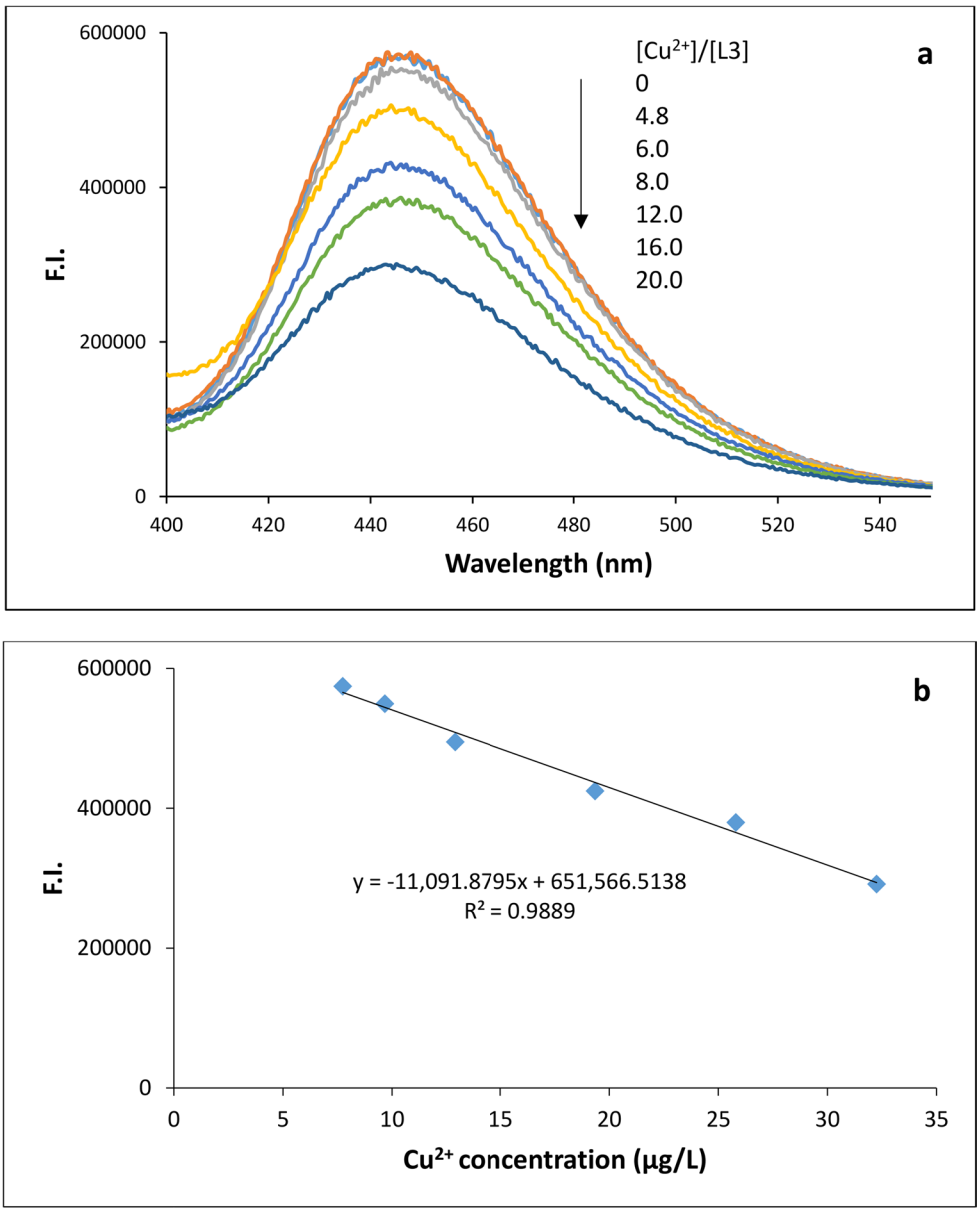

Fig. 2 Spectrofluorometric titration of Cu^{2+} ions using compound L3: (**a**) fluorescence spectrum of L3; (**b**) systematic decrease in fluorescence intensity at 449 nm with increasing Cu^{2+} concentration

[L3] = 0–20 µg/L. As the Cu^{2+} concentration increases, the fluorescence intensity of L3 at 449 nm decreases accordingly. This quenching effect can be attributed to the interaction between Cu^{2+} ions and L3, which *leads to a reduction in fluorescence intensity.*

As shown in Fig. 2b, there is a strong linear correlation (R^2 = 0.9889) between fluorescence intensity and Cu^{2+} concentration. The calibration curve (y = −11.09187x + 651.56651) indicates that L3 may be used as a sensitive and reliable fluorescent sensor for Cu^{2+} determination. Based on these results, a simple and reproducible method for Cu^{2+} quantification in aqueous samples was developed using L3.

Due to potential inaccuracies of results obtained with the external calibration curve, a modified standard addition method was employed for the determination of Cu^{2+} in spiked tap water samples using the L3 compound [26]. The fluorescence spectra of all solutions used in the standard addition method were recorded upon excitation at 330 nm (Fig. 3a). The emission intensities at 449 nm were plotted against the corresponding Cu^{2+} concentrations to form the calibration curve (Fig. 3b).

The Cu^{2+} concentration in the water sample was calculated using Eq. 1 by dividing the fluorescence intensity difference between the first and second tubes ($F - F_0$) by the slope of the calibration curve.

$$C_x = (F - F_0) / m \quad (1)$$

Where C_x is the Cu^{2+} concentration in the water sample, F is the fluorescence intensity at 449 nm for the solution in the first tube, and F_0 is the intensity for the solution in the second tube. m represents the slope of calibration graph.

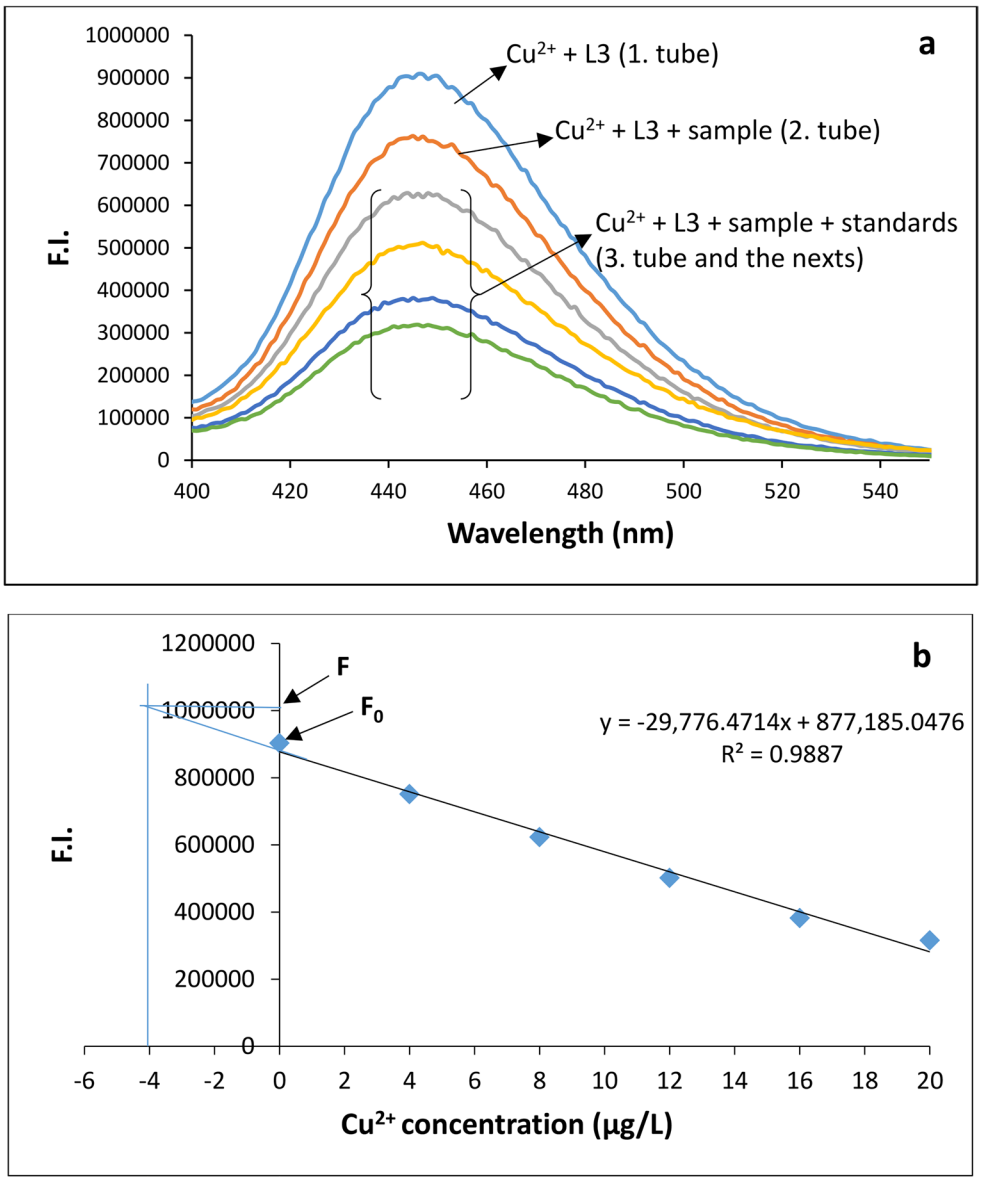

Fig. 3 Changes in the fluorescence spectra of Cu^{2+}-L3 complex during modified standard addition method (**a**), standard addition graph for Cu^{2+} determination (4 µg/mL) determination in tap water (**b**) (emission wavelength: 449 nm)

Table 1 Analytical performance data of the Cu^{2+} determination with L3 compound

Excitation wavelength (nm)	330
Emission wavelength (nm)	449
Limit of detection (µg/L)	0.98
Limit of quantification (µg/L)	2.92
Linear range (µg/L)	0–32
Constant Cu^{2+} concentration (µg/L)	2.0
Ligand concentration (mol/L)	5.0×10^{-8}
Ligand volume (mL)	2
Total volume (mL)	4
Solvent	ethanol: water (1:1)
Time before measurement	1–2 min.
Correlation coefficient (R^2)	0.9887
Precision (RSD, $N=3$) (%)	5.2-6.0

Alternatively, the Cu^{2+} concentration in the sample may also be estimated by extrapolation, as shown in Fig. 3b.

Analytical Performance of the Proposed Method

The linear range was determined under optimized conditions by observing a consistent and proportional decrease in the fluorescence intensity of the L3 compound with increasing Cu^{2+} concentrations, indicating a linear response within the tested range of 0–32 µg/L (Fig. 2b). According to the data presented in Table 1, the fluorescence intensity at 449 nm showed a linear correlation with Cu^{2+} concentration, with a correlation coefficient of $R^2 = 0.9887$, suggesting good linearity of the calibration curve.

The limit of detection (LOD) and limit of quantification (LOQ) were calculated based on the standard deviation obtained from eleven replicate measurements of blank samples. The LOD and LOQ values were calculated based on the IUPAC guidelines, using the equations $LOD = 3 \times \sigma/m$ and $LOQ = 9 \times \sigma/m$, where σ represents the standard deviation of eleven replicate measurements of the blank signal and m is the slope of the calibration curve. The accuracy of the proposed method was evaluated by spiking tap water samples with a known amount of Cu^{2+} and calculating the recovery rates. At a concentration level of 4.0 µg/L, the percentage error was found to be 5.58%, corresponding to a recovery rate of 94.42%. Each measurement was performed in triplicate. Precision was evaluated in terms of relative standard deviation (RSD, %) (RSD, %) for both intra-day and inter-day analyses of tap water samples spiked with 4.0 µg/L Cu^{2+}, yielding values of 5.2% and 6.0%, respectively.

Quenching Mechanism

The Stern–Volmer relationship is widely used to describe fluorescence quenching mechanisms and to investigate interactions between fluorophores and quenchers [27]. Fluorescence quenching occurs when the fluorescence intensity of a fluorophore decreases due to either collisional interactions (dynamic quenching) or ground-state complex formation (static quenching) with a quencher. The Stern–Volmer plot, which shows the ratio of fluorescence intensity in the absence (F_0) and presence (F) of quencher against quencher concentration, provides information about the quenching process. A linear plot typically indicates pure dynamic quenching, while non-linear behavior, such as upward curvature, may indicate the simultaneous presence of dynamic and static quenching mechanisms [26, 27].

The Stern–Volmer relationship was investigated to determine the nature of the interaction between Cu^{2+} and the L3 compound. The Stern–Volmer plot (Fig. 4) shows the variation of F_0/F as a function of Cu^{2+} concentration. As the

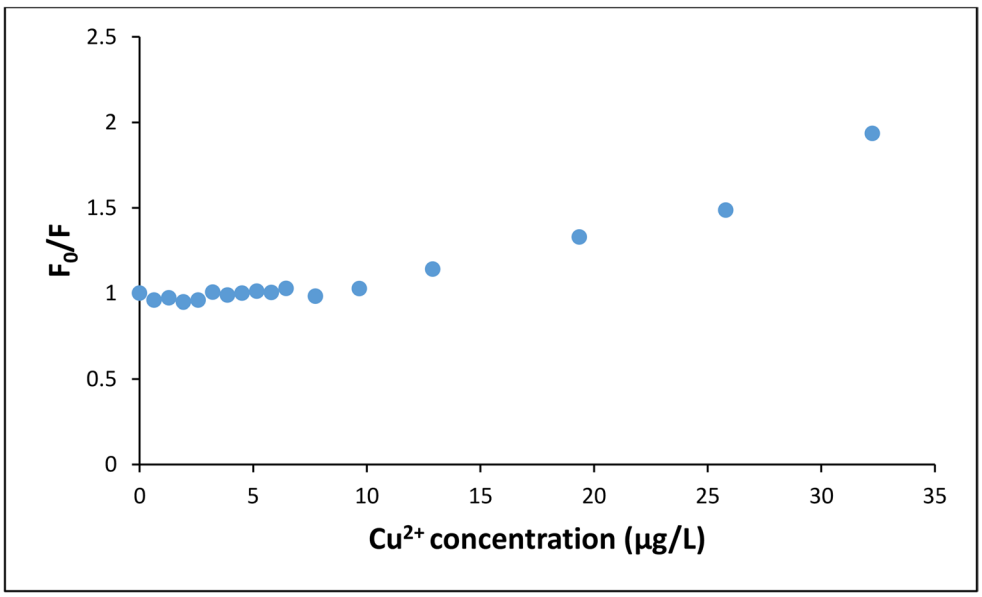

Fig. 4 Stern–Volmer plot of fluorescence quenching in Cu^{2+}-L3 system

Table 2 Comparison of methods including schiff bases for cu^{2+} detection in water in the literature

Sample	LOD (M)	Ref.
Lake water, tap water	1.25×10^{-8}	[38]
Environmental water	8.8×10^{-8}	[39]
Tap water, drinking water	1.94×10^{-7}	[40]
Lake water, well water, and seawater	3.9×10^{-8}	[41]
Tap water	2.5×10^{-7}	[42]
Tap water	1.5×10^{-8}	This work

Cu^{2+} concentration increases, suggesting that fluorescence quenching of L3 occurs in the presence of Cu^{2+} ions [36].

The intersection of the plot with the y-axis at unity ($F_0/F = 1$) supports the applicability of the Stern–Volmer relationship under the working conditions. At low concentrations, the linear profile of the plot suggests that static quenching is the primary mechanism, likely due to ground-state complex formation between L3 and Cu^{2+} ions [36]. The deviation from linearity observed at higher concentrations could indicate the involvement of additional quenching mechanisms or the formation of more complex species [26]. At higher concentrations, the upward deviation from linearity suggests that, in addition to static quenching, a dynamic quenching mechanism may also contribute to the process [37].

Comparison with fluorescence-based Methods Reported in the Literature

Table 2 summarizes and compares the detection limits (LOD) of Cu^{2+} ions achieved by various fluorescence-based methods applied to real water samples, including those employing Schiff base derivatives [38–42]. The previously reported LOD values typically range from 10^{-7} to 10^{-8} M. For example, Mohanasundaram et al. reported a LOD of 1.25×10^{-8} M in lake and tap water [38], while Bhaskar et al. achieved a LOD of 8.8×10^{-8} M in environmental water [39]. In contrast, the probe developed in this study exhibited a comparable LOD of 1.5×10^{-8} M in tap water, indicating a reasonable level of sensitivity. These findings highlight the efficiency of the proposed Schiff base probe and its promising application potential for Cu^{2+} detection in environmental monitoring.

Supplementary Information The online version contains supplementary material available at https://doi.org/10.1007/s10895-025-04543-0.

Acknowledgements The authors gratefully acknowledge the support of the Kafkas University Scientific Research Projects Coordination Unit (Project No. 2018-FM-42).

Author Contributions ÜTO, MO and ZO: Conceptualization, Investigation, Methodology, Formal analysis, Writing - orginal draft. AG: Investigation, Preparation, Writing - original draft.

Funding This work was supported by the Kafkas University Scientific Research Projects Coordination Unit (Grant number 2018-FM-42).

Data Availability No datasets were generated or analysed during the current study.

Declarations

Competing interests The authors declare no competing interests.

References

1. Ebenezer O, Oyetunde-Joshua F, Omotoso OD, Shapi M (2023) Benzimidazole and its derivatives: recent advances (2020–2022). Results Chem 5:100925. https://doi.org/10.1016/j.rechem.2023.100925
2. Wagih N, Abdel-Rahman IM, El-Koussi NA, Abuo-Rahma GE (2025) Anticancer benzimidazole derivatives as inhibitors of epigenetic targets: a review Article. RSC Adv 15:966–1010. https://doi.org/10.1039/d4ra05014b
3. Mahurkar ND, Gawhale ND, Lokhande MN, Uke SJ, Kodape MM (2023) Benzimidazole: a versatile scaffold for drug discovery and beyond – a comprehensive review of synthetic approaches and recent advancements in medicinal chemistry. Results Chem 6:101139. https://doi.org/10.1016/j.rechem.2023.101139
4. Natarajan R, Kumar P, Subramani A, Siraperuman A, Angamuthu P, Bhandare RR, Shaik AB (2024) A critical review on therapeutic potential of benzimidazole derivatives: a privileged scaffold. Med Chem 20(3):311–351. https://doi.org/10.2174/0115734064253813231025093707
5. Uriu-Adams JY, Keen CL (2005) Copper, oxidative stress, and human health. Mol Aspect Med 26:268–298. https://doi.org/10.1016/j.mam.2005.07.015
6. Gaetke LM, Chow-Johnson HS, Chow CK (2014) Copper: toxicological relevance and mechanisms. Arch Toxic 88:1929–1938. https://doi.org/10.1007/s00204-014-1355-y
7. Fukai T, Ushio-Fukai M, Kaplan JH (2018) Copper transporters and copper chaperones: roles in cardiovascular physiology and disease. Am J Phys Cell Phys 315:C186–C201. https://doi.org/10.1152/ajpcell.00132.2018
8. Binesh A, Venkatachalam K (2024) Copper in human health and disease: A comprehensivereview. J Biochem Mol Toxicol 38:e70052. https://doi.org/10.1002/jbt.70052
9. Mishra A, Shukla D, Vakhela K, Saraf M (2019) Copper: its biological role and toxicity. J Indian Bot Soc 98(1):26–36
10. Barnham K, Masters C, Bush A (2004) Neurodegenerative diseases and oxidative stress. Nat Rev Drug Discov 3:205–214. https://doi.org/10.1038/nrd1330
11. Gaggelli E, Kozlowski H, Valensin D, Valensin G (2006) Copper homeostasis and neurodegenerative disorders (Alzheimer's, prion, and parkinson's diseases and amyotrophic lateral sclerosis). Chem Rev 106(6):1995–2044. https://doi.org/10.1021/cr040410w
12. Yruela I (2009) Copper in plants: acquisition, transport and interactions. Func Plant Biol 36(5):409–430. https://doi.org/10.1071/FP08288
13. He ZL, Yang XE, Stoffella PJ (2005) Trace elements in agroecosystems and impacts on the environment. J Trace Elem Med Biol 19(2–3):125–140. https://doi.org/10.1016/j.jtemb.2005.02.010
14. Arslan Topal EI, Elitok Z (2018) Seasonal monitoring of Cu and Zn in the sewage sludge of Malatya advanced biological wastewater treatment plant. Int J Pure Appl Sci 4:51–60. https://doi.org/10.29132/ijpas.365425

15. Oltulu Ç, Daşman M (2024) Determination of toxic metals in some food supplements by ICP-MS. J Fac Pharm Ankara Univ 48:86–96. https://doi.org/10.33483/jfpau.1279257
16. Khan S, Ullah Q, Parveen H, Mukhtar S, Alzahrani K, Asad M (2021) Synthesis and photophysical investigation of novel imidazole derivative: an efficient multimodal chemosensor for Cu(II) and fluoride ions. J Photochem Photobiol Chem 406:113022. https://doi.org/10.1016/j.jphotochem.2020.113022
17. Diehl K (2022) A simple pyridine based fluorescent chemosensor for selective detection of copper ion. Spectrochim Acta Mol Biomol Spectrosc 265:120395. https://doi.org/10.1016/j.saa.2021.120395
18. Ömeroğlu İ, Şanko V (2023) A 'turn off' fluorescence sensor for fe^{2+}, fe^{3+}, and cu^{2+} ions based on novel pyrene-functionalized Chitosan. Turk J Anal Chem 5:50–60. https://doi.org/10.51435/turkjac.1302873
19. Karakuş E, Gunduz S, Liv L, Ozturk T (2020) Fluorescent and electrochemical detection of Cu (II) ions in aqueous environment by a novel, simple and readily available AIE probe. J Photochem Photobiol Chem 400:112702. https://doi.org/10.1016/j.jphotochem.2020.112702
20. Qi X, Jun EJ, Xu L, Kim SJ, Hong JSJ, Yoon YJ, Yoon J (2006) New BODIPY derivatives as OFF–ON fluorescent chemosensor and fluorescent chemodosimeter for cu^{2+}: cooperative selectivity enhancement toward cu^{2+}. J Org Chem 71:2881–2884. https://doi.org/10.1021/jo052542a
21. Elçin S, Deligöz H, Bhatti AA, Oguz M, Karakurt S, Yilmaz M (2016) Synthesis and evaluation of fluorescence properties of cu^{2+}selective azocalix[4]arenes and their application in living cell imaging. Sens Actuators B Chem 234:345–352. https://doi.org/10.1016/j.snb.2016.04.155
22. Yurtman Gündüz Z, Gündüz C, Özpınar C, Aydın Urucu O (2015) A novel schiffbase as a Cu(II) ion fluorescent sensor in aqueous solution. Spectrochim Acta Mol Biomol Spectrosc 136(C):1679–1683. https://doi.org/10.1016/j.saa.2014.10.066
23. Karuk Elmas ŞN, Arslan FN, Aydin D (2022) A novel ratiometric fluorescent and colorimetric sensor based on a 1,8naphthalimide derivative for nanomolar cu^{2+} sensing: smartphone and food applications. Analyst 147:2687–2695. https://doi.org/10.1039/D2AN00537A
24. Ravi V, Ramu E, Vijay K, Srinivas Rao A (2007) Zn-proline catalyzed selective synthesis of 1,2-disubstituted benzimidazoles in water. Chem Pharma Bull 55(8):1254–1257. https://doi.org/10.1248/cpb.55.1254
25. Perumal S, Mariappan S, Selvaraj S (2004) A microwave assisted synthesis of 2-aryl-1-arylmethyl-1H-1,3- benzimidazoles in the presences of K-10. Arkivoc. 46–51. https://doi.org/10.3998/ark.5550190.0005.807
26. Çağlar Y, Saka ET, Alp H, Kantekin H, Ocak M, Ocak Ü (2016) A simple spectrofluorimetric method based on quenching of a Nickel(II)phthalocyanine complex to determine iron (III). J Fluoresc 26:1381–1389
27. Gümrükçüoğlu A, Ocak M, Kolaylı S, Dinç S, Altin I, Gün S, Turgut Ocak Ü (2025) Spectrofluorometric determination of fe^{3+}, pd^{2+}, and sn^{2+} ions using carbon nanodots derived from hazelnut shells. Methods Appl Fluoresc 13(3). https://doi.org/10.1088/2050-6120/add1aa
28. Kowser Z, Rayhan U, Akther T, Redshaw C, Yamato T (2021) A brief review on novel pyrene based fluorometric and colorimetric chemosensors for the detection of cu^{2+}. Mater Chem Front 5:2173–2200. https://doi.org/10.1039/D0QM01008A
29. He G, Ma N, Li L, Xie C, Yang L, Xu J, Wang J (2019) A coumarinbased fluorescence probe for selective recognition of cu^{2+} ions and live cell imaging. J Sens 2814947. https://doi.org/10.1155/2019/2814947
30. Homocianu M, Hamciuc E, Hamciuc C (2025) Sensing of co^{2+} and cu^{2+} ions using dimethylaminofunctionalized poly(azomethine-1,3,4oxadiazole)s. J Fluoresc 35(5):3495–3505. https://doi.org/10.1007/s10895-024-03772-z
31. De Costa MDP, Jayasinghe WAPA (2004) Detailed studies on complexation behaviour and mechanism of fluorescence quenching of naphthalenelinked hydroxamic acid with transition metal ions by uvvisible and fluorescence spectra. J Photochem Photobiol Chem 162(2–3):591–598. https://doi.org/10.1016/S1010-6030(03)00419-2
32. Reshma R, Joseyphus R, Arish D, Reshmi Jaya RJ, Johnson J (2021) Tridentate imidazolebased schiff base metal complexes: molecular docking, structural and biological studies. J Biomol Struct Dyn 40(18):8602–8614. https://doi.org/10.1080/07391102.2021.1914171
33. Musikavanhu B, Liang Y, Xue Z, Feng L, Zhao L (2023) Strategies for improving selectivity and sensitivity of schiff base fluorescent chemosensors for toxic and heavy metals. Molecules 28:6960. https://doi.org/10.3390/molecules28196960
34. Sharma S, Chayawan, Debnath J, Sundar Ghosh K (2023) Method for highly selective, ultrasensitive fluorimetric detection of cu^{2+} and al^{3+} by schiff bases containing Ophenylenediamine and oaminophenol. Methods 217:27–35. https://doi.org/10.1016/j.ymeth.2023.06.013
35. Heck J, Metz F, Buchenau S, Teubner M, GrimmLebsanft B, Spaniol TP, Hoffmann A, Rübhausen MA, HerresPawlis S (2022) Manipulating electron transfer – the influence of substituents on novel copper guanidine Quinolinyl complexes. Chem Sci 13(28):8274–8288. https://doi.org/10.1039/d2sc02910c
36. Sogukomerogullari HG, Basaran E (2022) Synthesis and characterization of new hydrazone derivatives Fe(II), Co(II), Ni(II) and Cu(II) complexes. Süleyman Demirel univ. J Nat Appl Sci 26(2):216–222. https://doi.org/10.19113/sdufenbed.1031209
37. Rajapakshe BU, Li Y, Corbin B, Wijesinghe KJ, Pang Y, Abeywickrama CS (2022) Copperinduced fluorescence quenching in a bis[2(2′hydroxyphenyl)benzoxazole]pyridinium derivative for quantification of Cu^{2+} in solution. Chemosensors 10:382. https://doi.org/10.3390/chemosensors10100382
38. MohanasundaramM EKP, Saravanan J (2022) A dual sensor for fe^{3+} and cu^{2+} ions based on a new acylhydrazone derivative: synthesis, characterization and DFT studies. J Photochem Photobiol Chem 428:113850. https://doi.org/10.1016/j.jphotochem.2022.113850
39. Bhaskar C, Dey S (2019) Colorimetric and fluorometric chemosensor for the sequential detection of cu^{2+} and F^- ions in environmental samples. Inor Chem Commun 103:122–128. https://doi.org/10.1016/j.inoche.2019.03.041
40. Kumar M, Kumar D (2023) A highly selective schiff base fluorescent sensor for the detection of cu^{2+} in drinking water and living cells. J Photochem Photobiol Chem 438:114750. https://doi.org/10.1016/j.jphotochem.2023.114750
41. Tamizhselvi G, Karthikeyan M, Sakthivel P, Al-Hemaid FMA, Mohamed MAA (2024) A schiff base-based fluorescent sensor for highly sensitive detection of cu^{2+} in aqueous media and its application in environmental analysis. Spectrochim Acta Mol Biomol Spectrosc 308:124766. https://doi.org/10.1016/j.saa.2024.124766
42. Mohanasundaram M, Saravanan J (2021) A highly sensitive schiff base fluorescent sensor for cu^{2+}: real sample application and molecular Docking studies. Spectrochim Acta Mol Biomol Spectrosc 254:120395. https://doi.org/10.1016/j.saa.2021.120395